

# On increasing efficiency of hydraulic fracture simulation by using dynamic approach of modified theory

A.D. Stepanov, A.M. Linkov  
a.stepanov93@yandex.ru

## Abstract

The work aims to make a further step in using the computational advantages of the modified theory for efficient simulation of hydraulic fracturing. The step is made by solving the KGD problem in frames of the dynamic approach in non-normalized coordinates with using hypersingular elasticity operator. It is shown that the obtained system of ODE may be efficiently integrated by employing accelerated Runge-Kutta or Adams methods. The approach developed provides acceptable accuracy for Newtonian and thinning fluids used in practice. We conclude that it may be extended to 3D problems.

## 1 Introduction

Numerical simulation is an important means to improve understanding and to control hydraulic fracturing (HF), which is widely used for many engineering purposes. They include oil, gas and heat recovery, CO<sub>2</sub> sequestration, waste disposal, excavation of hard rock, preconditioning in mines, etc. Despite numerous studies have been performed during the last four decades (see e. g. reviews in [1], [6], [16]), numerical simulation of truly 3D HF problems still remains "a formidable task" (see [2], p. 147). There is need to "dramatically speed up" simulators (see [1], p. 754). It is a challenge to radically improve HF simulation.

The recent findings [5, 6, 7, 10] suggest a means to meet the challenge. They are summarized in the modified formulation of the HF problem. The analytical and computational advantages of the modified formulation have been demonstrated by obtaining new analytical solutions and very accurate and computationally efficient numerical algorithms for 1D problems (e.g., [6], [8] - [10], [16]). These results confirm that drastic progress may be achieved in numerical simulation of 2D fractures in the 3D space.

Emphasize however that efficient techniques open by the modified formulation for *tracing* a moving fracture front, have not completely overcome the remaining difficulties caused by a) strong non-linearity of the problem, b) non-integrable singularity of the pressure gradient at points of the front, and c) the fact that, for a general 3D

problem, the dependence between the opening and net-pressure involves hypersingular operator. The cited 1D solutions have employed *ad hoc simplifications*, which being available in 1D cases, are unavailable in general 3D problems. Therefore, it is reasonable to re-visit the classical 1D problems for developing tools, which do not employ the *ad hoc* simplifications and may be extended to 3D problems.

The present work aims to make a step in this direction. To the date, except for the paper [5] considering the PKN [12], [13] model, the computational advantages of the modified theory have been confirmed by calculations only when the PKN and KGD [3],[4] problems were solved in coordinates *normalized* by the fracture length. This excluded singularity of the temporal derivative of the opening at the fracture tip. However, such beneficial normalizing is unavailable in 3D problems because, for them, the fracture front is composed of continuum of points. Thus, it is of value to solve the KGD problem in frames of the modified theory in *global* coordinates without using the normalizing. Furthermore, having in mind extensions to 3D problems, it is reasonable to employ *hypersingular* operator, which expresses the pressure via the opening, rather than its *weakly singular* inversion. The inversion, although beneficial when there is an analytical expression for the inverse operator (e.g. [8], [16]), is not available in an analytical form in general.

Summarizing, the objective of the paper is to develop methods, based on the modified formulation, which provide accurate, computationally efficient and stable solution of the KGD problem with two features, which suggest extensions to 3D problems:

- (i) the solution is found in the global rather than normalized coordinates,
- (ii) the solution is obtained by using the direct (hypersingular) rather than inverse (weakly singular) elasticity operator.

The second feature also opens the possibility to employ the *dynamic* approach in time stepping as an alternative to the schemes of the Crank-Nicolson type, which, strictly speaking, require  $\varepsilon$ -regularization. Below to demonstrate the extended options, we employ the dynamic approach. It consists of complementing the system of ODE, obtained after spatial discretization, with the speed equation, in which its r. h. s. is evaluated by using the universal asymptotic umbrella [7]. We reach the goal by developing numerical schemes, which show high efficiency and which may be promptly extended to 3D problems. The accuracy control is performed by the comparison of the results obtained with the self-similar solution found to the accuracy of four correct significant digits, at least. We focus on the comparison of the key quantities, which are the opening at the inlet and the fracture length. The time range considered covers two decimal orders (in practice, it corresponds to the time growth from first minutes to first hours what is typical for HF treatments). It is also established that the methods developed are applicable for Newtonian, as well as for thinning fluids, used in practice.

## 2 Problem formulation

We consider the plane KGD problem of HF for the practically important case when the rheology of a fracturing fluid is prescribed by the power-type dependence:

$$\tau = M\dot{\gamma}^n, \tag{1}$$

where  $\tau$  is the shear stress,  $\dot{\gamma}$  is the shear strain rate,  $M$  is the consistency index,  $n$  is the fluid behavior index. For a Newtonian fluid,  $n = 1$ ; for a perfectly plastic fluid,  $n = 0$ ; for thinning fluids,  $0 < n < 1$ .

We use the modified formulation of the problem. In contrast with the conventional formulation, it employs the particle velocity  $v$  instead of the flux, the speed equation (SE) instead of the global mass balance and the universal asymptotic umbrella to prescribe the r. h. s. of the SE.

The equations for a *fluid* include the *continuity equation*:

$$\frac{\partial w}{\partial t} = -\frac{\partial (wv)}{\partial x} - q_l, \tag{2}$$

and the Poiseuille-type *movement equation*:

$$v = \left[ \frac{w^{n+1}}{\mu'} \left( -\frac{\partial p}{\partial x} \right) \right]^{1/n}, \tag{3}$$

where  $w$  is the fracture opening,  $p$  is the net-pressure,  $q_l$  is the term accounting for fluid leak-off into formation,  $\mu' = \theta M$ ,  $\theta = 2 \left[ \frac{2(2n+1)}{n} \right]^{1/n}$ .

We neglect a small lag and consider the physically consistent case when singularity, if it is generated by the leak-off term at the front, is not too strong to distort predominantly in-plane flow within the fracture. Then, as shown in [7], the SE has the form following from the Reynolds transport theorem. Specifically, in the considered case of a power-law fluid, the particle velocity  $v$  tends to the propagation speed  $v_*$  at the fracture tip  $x = x_*$ , so that the *speed equation* is:

$$\frac{dx_*}{dt} = v_* = \lim_{x \rightarrow x_*} \left( -\frac{w^{n+1}}{\mu'} \frac{\partial p}{\partial x} \right)^{1/n}. \tag{4}$$

The opening  $w$  is not prescribed in advance. For *elastic rocks*, it is defined by the equation of the elasticity theory, connecting the opening and net-pressure. Except for the particular cases of straight and penny-shaped factures, when there exists weakly singular analytical inversion, the explicit form of the equation contains hypersingular integral with density equal to the opening. The net-pressure is proportional (with known factor) to the integral. In the considered 1D problem, taking into account that the problem is symmetric about the origin ( $w(-x) = w(x)$ ,  $p(x) = p(-x)$ ), the *elasticity equation* is:

$$p(x, t) = -\frac{E'}{4\pi} \int_0^{x_*} \left[ \frac{1}{(\xi - x)^2} + \frac{1}{(\xi + x)^2} \right] w(\xi, t) d\xi, \quad 0 \leq x \leq x_*, \tag{5}$$

where  $E' = \frac{E}{1-\nu^2}$ ,  $E$  is Young's modulus,  $\nu$  is Poisson's ratio. The density  $w(x, t)$  is assumed to belong to the class of functions equal to zero at the fracture tip:

$$w(x_*, t) = 0. \tag{6}$$

The possibility of the fracture propagation is defined by the *fracture criterion* of linear fracture mechanics

$$K_I = K_{IC}, \tag{7}$$

where  $K_I$  is the stress intensity factor (SIF),  $K_{IC}$  is its critical value. Then equations of the elasticity theory yield for the opening near the tip  $x = x_*$ :

$$w(x, t) = \sqrt{\frac{32}{\pi} \frac{K_{IC}}{E'}} \sqrt{x_* - x} + O((x_* - x)^\alpha), \tag{8}$$

where  $1 \geq \alpha > 1/2$ . The exact asymptotic behavior of the opening, pressure and their spatial derivatives near the fracture front is completely defined by the propagation speed [7]. We focus on the viscosity dominated regime, when the major resistance to the fracture propagation is caused by the fluid viscosity  $\mu'$  rather than fracture toughness  $K_{IC}$ . This regime is typical for HF propagation (see, e. g. [14]). For it, fracture toughness may be neglected ( $K_{IC} = 0$ ). Then the first term on the r. h. s. of (8) vanishes and asymptotic dependence of the opening on the propagation speed becomes [7]:

$$w = A_\mu(\alpha) v_*^{1-\alpha} [(x_* - x)^\alpha], \tag{9}$$

where  $\alpha = 2/(n + 2)$ ,  $A_\mu(\alpha) = [(1 - \alpha) B(\alpha)]^{-\frac{\alpha}{2}}$ ,  $B(\alpha) = \frac{\alpha}{4} \cot[\pi(1 - \alpha)]$ . In view of the asymptotic umbrella (9), the SE (4) becomes

$$\frac{dx_*}{dt} = v_* = [A_\mu(\alpha)]^{-\frac{1}{1-\alpha}} \lim_{x \rightarrow x_*} \left[ \frac{w(x)}{(x_* - x)^\alpha} \right]^{\frac{1}{1-\alpha}}. \tag{10}$$

The *boundary conditions* (BC) for the partial differential equations (2) and (3) are as follows. One of them is the condition of zero opening at the front (6). It is satisfied automatically by using the opening in the mentioned class of functions. In particular, accounting for the asymptotics (9) automatically meets the condition of zero opening at the front. The second BC is the condition of the prescribed influx  $Q = 2q_0$  at the inlet ( $x = 0$ ). In terms of the particle velocity it is:

$$w(0) v(0+) = q_0. \tag{11}$$

Using the limit  $v(0+)$  of the velocity from right accounts for the fact that the velocity is discontinuous at the source point ( $v(0+) = -v(0-)$ ). Consequently, the influx  $Q_0$  is equally distributed between the left and right parts of the fracture, so that  $q_0 = Q/2$ .

The *initial conditions* (IC) assign the opening  $w_0(x)$  and the fracture length  $x_{*0}$  at an initial moment  $t_0$  of time:

$$\begin{aligned} w(x, t_0) &= w_0(x) & |x| &\leq x_*(0), \\ x_*(0) &= x_{*0}. \end{aligned} \tag{12}$$

We need to solve equations (2), (3), (5) in the class of functions  $w(x, t)$  with the asymptotics (9), under the BC (11), the IC (12) and with the propagation speed  $dx_*/dt$  defined by (10).

### 3 Scaling

We introduce the normalizing opening  $w_n$

$$w_n = \left( t_s \frac{E'}{\mu'} \right)^{\frac{1}{n+2}} \tag{13}$$

to exclude the elasticity  $E'$  and viscosity  $\mu'$  constants from the movement and elasticity equations. The constant  $t_s$  in (13) denotes a time-scaling factor, which may be chosen for convenience. Specifically, when the shear strain rate in (1) is measured in the usual unit  $1/s$ , then taking  $t_s = 60^n$  actually transforms the viscosity to time units of minutes. Then the particle velocity, leak-off term, the propagation speed, the influx in the source and the initial time may be specified with time measured in minutes. This is more convenient than tracing a HF propagation with time measured in seconds. In particular, with  $t_s = 60^n$ , the initial time  $t_0 = 1$  corresponds to 1 minute. Accordingly, hundred-fold greater time  $t = 100$  corresponds to 100 minutes what has the usual order of HF treatment time. Therefore, in further calculations we may consider the problem when the time changes in the range from first to hundreds units.

The normalized variables are:

$$\begin{aligned} w' &= \frac{w}{w_n} & p' &= \frac{p}{w_n E'} \\ q'_l &= \frac{q_l}{w_n} & w'_0 &= \frac{w_0}{w_n} \\ q'_0 &= \frac{q_0}{w_n}. \end{aligned} \tag{14}$$

In terms of the normalized quantities (14), marked by the primes, the system of equations (2), (3), (5), the SE (10), boundary conditions (6), (11) and initial conditions (12) keep their form with the only difference: now the constants  $E'$  and  $\mu'$  are set unit. From now on to simplify notation, we write the normalized variables omitting primes.

### 4 Numerical solution by using dynamic approach

In this paper, we employ the pressure explicitly defined via the opening by hyper-singular operator. This suffices applicability of the *dynamic approach* [7], [9], [10].

It consists of reducing the problem to a complete system of ordinary differential equations (ODE) in time.

The complete system is obtained as follows. We start with an interval of the length  $L$ , exceeding, for certainty and convenience two-fold, the initial fracture half-length  $x_{*0}$ . On the interval, we spatially discretize the r. h. s. of equations (2), (3), (5) by using finite differences for PDE (2) and (3) and appropriate quadrature rules for the hypersingular integral in (5). An approximation of the opening and velocity involves a *fixed number*  $M + 1$  values  $w_i = w(x_i, t), v_i = v(x_i, t)$  at  $M + 1$  points  $x_i$  with zero values of the opening and velocity at points *ahead* of the fracture front ( $x \geq x_*$ ). Therefore, the r. h. s. of discretized continuity equation is actually set zero at nodal points ahead of the front. The hypersingular integral (5) provides the nodal values  $p_i$  of the pressure *behind* the front expressed via  $M + 1$  values of the opening. Then substitution of the found  $p_i$  into discretized movement equation (3) gives the nodal values  $v_i$  of the particle velocity *behind* the front expressed via  $w_i$ . Thus the discretized r. h. s. of continuity equation (2) becomes expressed via the nodal values  $w_i$  of the opening. Equating it to the l. h. s. of (2), represented by the time derivatives  $\partial w_i / \partial t$ , at  $M$  nodal points yields  $M$  ODE in  $M$  unknowns  $w_i$ . (There is no sense to include the last  $M + 1$ -th point, where the opening and its temporal derivative are always zero, because the interval is doubled when the front reaches this point). Still, the obtained system of ODE is not complete because it contains the unknown half-length  $x_*(t)$ , which enters through the elasticity equation. The SE gives the needed additional equation. Indeed, the time derivative  $dx_*/dt$  is defined via the opening by the SE (10). Hence, by adding the SE to the ODE, obtained from the continuity equation, we arrive at a complete system of  $M + 1$  ODE with  $M + 1$  unknowns:  $M$  nodal openings  $w_i$  plus the fracture half-length  $x_*$ .

We follow this line by using the same finite differences for spatial derivatives and quadrature rules for hypersingular integral as those used in [9]. However, in contrast with [9], we employ non-normalized spatial coordinates to make possible an extension to 3D problems. It is easy to show that in non-normalized coordinates, the temporal derivative of the opening is singular as  $O((x_* - x)^{\alpha-1})$  at the fracture front. As noted in Introduction, this may unfavorably influence the accuracy of numerical results.

As mentioned, we start with an interval of the length  $L$  two-fold greater than the initial fracture half-length:  $L = 2x_{*0}$ . Later on, when the current fracture front  $x_*(t)$  reaches end point  $x = L$ , the length  $L$  is doubled and the problem becomes similar to that at the start of calculations.

We use a standard mesh with  $M + 1$  nodes on the interval  $L$ . The first node is always placed at the origin ( $x = 0$ ). Next nodes are located successively at distances  $\Delta x = L/M$  one from another:  $x_i = x_{i-1} + \Delta x$  ( $i = 2, \dots, M + 1$ ). The intermediate points are  $x_{i-1/2} = x_i - \Delta x/2$ , ( $i = 2, \dots, M + 1$ ) and, equivalently,  $x_{i+1/2} = x_i + \Delta x/2$  ( $i = 1, \dots, M$ ). The position of the front  $x = x_*$  is known on each current time step. It serves to find the number  $i_*$  of the node, which being ahead of the front is closest to it. Since the openings and velocities are zero at nodes ahead of the front, we set  $w_i = 0, v_i = 0$  for  $i = i_*, \dots, M + 1$ . The last node with non-zero opening has the number  $i_* - 1$ .

The nodal values of the pressure behind the front are found by using piece-wise

constant approximation of the opening in the hypersingular integral (5):

$$-\frac{4\pi}{E'}p_i = \sum_{j=1}^{M+1} A_{ij}w_j \quad i = 1, \dots, i_* - 1, \quad (15)$$

where  $A_{ij} = \frac{1}{\tau_j - x_i} - \frac{1}{\tau_{j+1} - x_i} + \frac{1}{\tau_j + x_i} - \frac{1}{\tau_{j+1} + x_i}$ , with  $\tau_1 = 0, \tau_2 = \Delta x/2, \tau_M = x_{M+1} - \Delta x/2, \tau_{M+1} = x_{M+1}$ , and  $\tau_j = x_{j-1/2}$  for  $j = 2, \dots, M - 1$ ; to avoid dividing by zero, the first collocation point  $x_1$  is taken slightly moved from the origin as  $x_1 = 0.0000001\Delta x$ . Note that the influence coefficients  $A_{ij}$  are inversely proportional to  $\Delta x$ . Hence, they may be evaluated by scaling the coefficients of a standard square matrix  $A_0$  of order  $M + 1$ , calculated in advance for a particular value of  $\Delta x$ , say,  $\Delta x_u = 1/M$ . This corresponds to the unit interval of integration. Then for a current  $\Delta x = L/M$ , the coefficients of  $A_{ij}$  are obtained simply by dividing coefficients of the matrix  $A_0$  by  $L$ .

The velocities behind the front are evaluated as follows. At the first node, the velocity is:

$$v_1 = (w_1^{n+1} \frac{p_1 - p_2}{\Delta x})^{1/n}.$$

At the point  $i_* - 1$  closest to the front, the velocity is calculated by using its known asymptotic behavior:

$$v_{i_*-1} = v_*[1 + a_v(1 - x_{i_*-1}/x_*)],$$

where  $a_v = -n/[(n+1)(n+4)]$ , and the propagation speed  $v_* = dx_*/dt$  is found by using the asymptotic umbrella (10) as

$$\frac{dx_*}{dt} = [A_\mu(\alpha)]^{-\frac{1}{1-\alpha}} \left[ \frac{w_{i_*-1}}{(x_* - x_{i_*-1})^\alpha} \right]^{\frac{1}{1-\alpha}}. \quad (16)$$

At other points on the fracture ( $i = 2, \dots, i_* - 2$ ), the velocity is found by using the finite difference equation suggested in [9] to account for strong singularity of the pressure near the front:

$$v_i = \left[ w_i^{n+1} \frac{p_{i-1} - p_{i+1}}{\Delta f(x_{i-1}, x_i, x_{i+1})} \right]^{\frac{1}{n}}, \quad (17)$$

where  $\Delta f = \frac{(x_* - x_i)^{\alpha(n+1)}}{\alpha(n+1)-1} \left[ \frac{1}{(x_* - x_{i+1})^{\alpha(n+1)-1}} - \frac{1}{(x_* - x_{i-1})^{\alpha(n+1)-1}} \right]$ . Thus, the openings and velocities become known at each node of the fixed mesh. They are used in finite differences representing the r. h. s. of continuity equation (2). At the first node, continuity equation is written by taking into account the BC (10) of prescribed influx  $Q$ . For certainty, the latter may be set unit ( $Q = 1$ ), consequently,  $q_0 = 1/2Q = 1/2$ . Continuity equation for the first node yields the ODE:

$$\frac{dw_1}{dt} = \frac{3q_0 - (4w_2v_2 - w_3v_3)}{2\Delta x}. \quad (18)$$

At following nodes up to that with the number  $i_*$ , the ODE are

$$\frac{dw_i}{dt} = \frac{-w_{i+1}v_{i+1} + w_{i-1}v_{i-1}}{2\Delta x}. \quad (19)$$

For nodes with numbers exceeding  $i_*$ , the nodal openings and velocities are zero; consequently, the r. h. s. of continuity equation are zero, as well, and the ODE are:

$$\frac{dw_i}{dt} = 0. \quad (20)$$

The complete dynamic system is obtained by adding the SE (16) to the  $M$  ODE (18)-(20), generated by continuity equation. The resulting system of ODE (18)-(20), (16) is solved under the discretized IC (11):

$$\begin{aligned} w_i(t_0) &= w_{i0} & i &= 1, \dots, M \\ x_* &= x_{*0}. \end{aligned}$$

Herein  $w_{i0}$  and  $x_{*0}$  are known numbers; for nodes ahead of  $x_{*0}$ , the initial openings are set zero:  $w_{i0} = 0$  when  $x_i > x_{*0}$ .

The complete system of ODE may be solved by standard methods like those by Euler, Runge-Kutta, Adams, etc. The coordinate  $x_*$  of the propagating front grows with increasing time. When it reaches the prescribed length  $L$ , the latter is doubled. Thus the interval again becomes equal to the doubled  $x_*$ . We keep the same number  $M + 1$  of nodes for the doubled interval. Then the mesh size  $\Delta x$  is also doubled. If taking  $M$  even ( $M = 2N$ ), odd nodes of the previous mesh become current nodes of the new mesh. The openings at these nodes are known; the current fracture half-length  $x_*$  is also known. Hence, we have the same system as that at the beginning of integration for previous  $L$ , with known initial values of nodal openings, with known half-length, and with doubled  $\Delta x$ . Since the mesh size  $\Delta x$  is increased, the time step may be also increased without loss of stability of an explicit scheme of integration.

## 5 Numerical results

We implemented the approach described by using two methods of time stepping: Runge-Kutta (R-K) of fourth order (without and with acceleration) and Adams. This tended to distinguish that method which provides stable accurate results with minimal time expense. A proper choice may serve for extending the approach to 3D HF problems.

We set  $Q_0 = 1$  ( $q_0 = 1/2$ ) and used various number of nodes:  $M + 1 = 21, 41, 61$  and 81. In accordance with Sec. 3, the time range considered was from the initial time  $t_0 = 1$  to the final time  $t_{fin} = 100$  of conditional time units. The range covers the usual time of a HF treatment. When using the R-K method, the time step  $\Delta t$  was chosen small enough to guarantee stability. Since the stability condition involves the ratio  $\Delta t/\Delta x^2$ , the time step could be increased with growing mesh size  $\Delta x$ . Calculations by the R-K method were performed either with a fixed time step (without acceleration), or with time step doubled when the mesh size was doubled (with acceleration). To further decrease the time expense, we employed the Adams

inexplicit predictor-corrector method with iterations at a time step. The accuracy of the calculations was checked by comparison with the self-similar bench-mark solution, obtained to the accuracy of four significant digits, at least. To make the comparison applicable at any time step, the initial conditions (12) at  $t_0 = 1$  were assigned as those corresponding to the self-similar solution at this instant. The typical numerical results obtained for a Newtonian fluid ( $n = 1$ ) are illustrated by Figure 1.

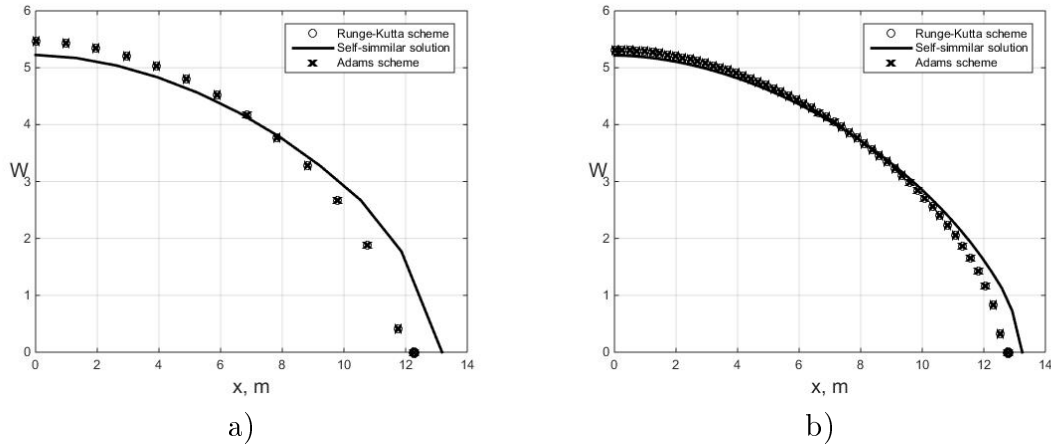


Figure 1: Computational results at time  $t_{fin} = 100$  for a)  $M + 1 = 21$  and b)  $M + 1 = 81$

It presents distributions of the opening along the fracture half-length at the final time  $t_{fin} = 100$  for  $M + 1 = 21$  (Figure 1a) and  $M + 1 = 81$  (Figure 1b) nodes. The last points at the  $x$ -axis correspond to the final half-length  $x_*$ . For comparison, the bench-mark self-similar solution is shown by the solid lines. It appears that for a quite coarse mesh with merely 21 nodes at the interval of the length  $2x_*$ , the error of the opening at the source is 3.7%, and the error of the half-length is 6.9%. For  $M + 1 = 41$  nodes, the errors become 2.0% and 4.9%, respectively. For  $M + 1 = 81$  nodes, they are 1.4% and 3.0%. As could be expected, these errors are greater than those reported in the paper [9], where the same meshes were used in the normalized coordinates. Then the error of the final half-length  $x_*$  did not exceed 0.94% even for  $N + 1 = 21$  nodes. The growth of errors is explained by the fact that for non-normalized coordinates, the temporal derivative  $\partial w / \partial t$  is singular as  $O((x_* - x)^{\alpha-1})$  at the front, while in normalized coordinates it is non-singular being equal to zero ( $\partial w / \partial t = 0$ ) at the front. Surely, the error may be decreased by more accurate integration of the elasticity equation and by direct accounting for the singularity discussed.

From Figure 1, it can be also seen that there is no significant differences in the accuracy of integration by the R-K and Adams methods. Hence, we may turn to the comparison of their computational efficiency. The calculations by the R-K method without acceleration with  $M + 1 = 41$  nodes required 1 hour to cover the range from  $t_0 = 1$  to  $t_{fin} = 100$  at a conventional laptop in the Matlab environment. Using acceleration drastically decreased this time; it became 10 minutes. Employing the Adams scheme additionally decreased the time to 5 minutes. Calculations with

using FORTRAN required two-fold less time when employing arithmetics of double precision. Therefore, in the problem considered, the accelerated R-K method is acceptable, while the Adams method appears superior over it.

The approach developed has been tested for thinning fluids ( $0 < n < 1$ ), as well. We could see that, similar to using the normalized coordinates [9], the accuracy notably decreased when the behavior index  $n$  approached zero. The reason is clear from equations (3) and (4). They contain the degree  $1/n$ , which tends to infinity when  $n$  goes to zero. This tremendously magnifies even small errors in the base of the exponent. Therefore for small  $n$ , the computational algorithm should be modified. It can be done by raising (3) and (4) to the degree  $n$  and expanding into Taylor's series in  $n$ . We do not employ this option, because in practice the behaviour index is not close to zero. Normally it exceeds the value 0.5 [11], for which the approach in the form described in the previous section provides results with acceptable accuracy. Specifically, for  $n = 0.5$ , when using the mesh with  $M + 1 = 41$  nodes, the errors of the opening at the source and of the half-length are 3.9% and 2.6%, respectively.

## 6 Conclusion

Summarizing, we conclude that the approach developed is efficient when solving the HF problem in global coordinates with using direct (hypersingular) elasticity operator. In the time range typical for HF treatments, integration of the obtained system of ODE may be efficiently performed by employing accelerated R-K or Adams methods; the latter looks superior over the former. It is shown that the approach provides acceptable accuracy for Newtonian and thinning fluids used in practice. The results imply that it may be successfully extended to 3D problems of hydraulic fracturing.

## Acknowledgement

*The authors highly appreciate the support of the Russian Scientific Fund (Grant # 15-11-00017)*

## References

- [1] J. Adachi, E. Siebrits, A. Pierce, J. Desroches. Computer simulation of hydraulic fractures. *Int. J. Rock Mech. Mining Sci.*, 44, No 5 (2007) 739.
- [2] E. Detournay, A. Peirce. On the moving boundary conditions for a hydraulic fracture. *Int. J. Eng. Sci.*, 84 (2014) 147.
- [3] J. Geertsma, F. de Klerk. A rapid method of predicting width and extent of hydraulically induced fractures. *J. Pet. Tech.*, 21 (1969) 1571.
- [4] S. A. Khristianovich, V. P. Zheltov. Formation of vertical fractures by means of highly viscous fluid. *Proc. 4-th World Petroleum Congr. Rome (1955)* 579.

- 
- [5] A. M. Linkov. Speed equation and its application for solving ill-posed problems of hydraulic fracturing. *Doklady Physics*, 56 (2011) 436.
- [6] A. M. Linkov. On efficient simulation of hydraulic fracturing in terms of particle velocity. *Int. J. Eng. Sci.*, 52 (2012) 77.
- [7] A. M. Linkov. The particle velocity, speed equation and universal asymptotics for the efficient modelling of hydraulic fractures. *J. Appl. Math. Mech.*, 79 (2015) 54.
- [8] A. M. Linkov. Solution of axisymmetric hydraulic fracture problem for thinning fluids. *J. Appl. Math. Mech.*, 80 (2016) 208.
- [9] A. M. Linkov. Solution of plane hydraulic fracture problem by Runge-Kutta method under arbitrary initial conditions. *Russian Mining Science*, 2 (2016). In print.
- [10] G. Mishuris, M. Wrobel, A. Linkov. On modeling hydraulic fracture in proper variables: Stiffness, accuracy, sensitivity. *Int. J. Eng. Sci.*, 61 (2012) 10.
- [11] C. Montgomery. Key-Note lecture: Fracturing fluids. Proc. Int. Conf. HF-2013 "Effective and Sustainable Hydraulic Fracturing ", Brisbane, Australia, 20–22 May 2013, A. P. Bungler et al. (eds), Croatia, InTech (2013) 3.
- [12] R. P. Nordgren. Propagation of a vertical hydraulic fracture. *Soc. Pet. Eng. J.*, 12 (1972) 306.
- [13] T. K. Perkins , L. R. Kern. Widths of hydraulic fractures. *J. Pet. Tech.*, 13, No 9 (1961) 937.
- [14] A. A. Savitski, E. Detournay. Propagation of a penny-shaped fluid-driven fracture in an impermeable rock: asymptotic solutions. *Int. J. Solids Structures*, 39 (2002) 6311.
- [15] D. A. Spence, P. W. Sharp. Self-similar solutions for elastohydrodynamic cavity flow. *Proc. Roy. Soc. London, Ser. A.*, 400, No 819 (1985) 289.
- [16] M. Wrobel, G. Mishuris. Hydraulic fracture revisited: Particle velocity based simulation. *Int. J. Eng. Sci.*, 94 (2015) 23.
- A. D. Stepanov, Institute of Problems of Mechanical Engineering RAS, 61, Bol'shoy pr. V.O., St. Petersburg, 199178, Russia*
- A. M. Linkov, Institute of Problems of Mechanical Engineering RAS, 61, Bol'shoy pr. V.O., St. Petersburg, 199178, Russia*